

Search for Unbound States in He^3 through $\text{Li}^6(p,\alpha)^\dagger$

DAVID K. OLSEN AND RONALD E. BROWN

John H. Williams Laboratory of Nuclear Physics, University of Minnesota, Minneapolis, Minnesota 55455

(Received 20 August 1968)

The shape of the α -particle continuum from the $\text{Li}^6(p,\alpha)$ reaction at a proton energy of 20.0 MeV (lab) has been investigated for structure due to excited states of He^3 . α -particle spectra were measured with thin surface-barrier detectors from 15° to 85° (lab) in steps of 5° . The maximum He^3 excitation energy which could have been observed with this experimental technique depended upon the lab angle and varied from 14.3 to 10.1 MeV. In order to continuously monitor the target composition, protons elastically scattered at 90° (lab) were observed simultaneously with the α -particle spectra. No clear structure attributable to the formation of excited states of He^3 was observed. In particular, an upper limit of 300 $\mu\text{b}/\text{sr}$ (lab) can be placed on the differential cross section at 20° (lab) for the excitation of a 12-MeV state in He^3 having a natural width of 0.9 MeV (c.m.).

I. INTRODUCTION

RECENTLY there has been considerable interest in the possible existence of states of the mass-3 system other than the ground states of He^3 and H^3 . Many experimental and theoretical investigations concerned with this possibility have been reported, and some of this work is listed in Ref. 1. In particular, the $\text{He}^3(p,p')$ study at 30.2 MeV of Kim *et al.*,² in which they appeared to have found evidence for states in He^3 having a width of about 0.9 MeV and occurring at excitation energies of 8.2, 10.2, and 12.6 MeV, has stimulated much activity directed toward a search for excited states of He^3 . The experiment we report here is such a search.³ In general, the result of these searches has been that no excited states in He^3 have been observed, and, if any do exist in the energy ranges investigated, then they must have widths significantly larger than those indicated by Kim *et al.*² After the present experiment was completed, two groups—Mancusi, Jones, and Ball⁴ and Austin, Benenson, and

Paddock⁵—reported the results of $\text{He}^3(p,p')$ experiments near 30 MeV. Neither group sees any evidence for the structure which appeared in the proton spectra of Kim *et al.*²

We report here a search for He^3 excited states by means of an examination for structure of the α -particle continuum produced in the $\text{Li}^6(p,\alpha)$ reaction. It should be mentioned that this reaction would be expected to strongly excite only states in He^3 having isospin $\frac{1}{2}$, whereas the $\text{He}^3(p,p')$ reaction, for example, should excite states having an isospin of either $\frac{1}{2}$ or $\frac{3}{2}$. We have observed the α -particle continuum at 15 lab angles between 15° and 85° . The highest He^3 excitation which we could have observed was 14.3 MeV at 40° (lab). We have found no evidence at any angle for structure in the α -particle continuum which could be clearly identified with the existence of excited states of He^3 .

II. EXPERIMENTAL APPARATUS

A. General Facilities

The experiment was performed using a 20.0-MeV proton beam produced by the MP tandem Van de Graaff accelerator at the University of Minnesota. After undergoing energy analysis, the beam was steered and focused onto a target placed in a scattering chamber,⁶ which contains two independently rotatable turntables on which detectors were mounted. After passing through the target, the beam was collected in a 165-cm-long, 10-cm-diam electrostatically shielded Faraday cup.

B. Detectors

The detector assemblies used were of two types: one for α -particle detection and one for proton detection. Three α -particle detectors were used simultaneously. Each was a surface-barrier type with a nominal thickness of 300 μ at a full bias voltage of 75 V and had a sensitive area of 5×15 mm. It was necessary to operate these detectors at reduced biased voltage in order to obtain a sensitive region thin enough so that the α

[†] Work supported in part by the U. S. Atomic Energy Commission.

¹ V. Ajdacić, M. Cerineo, B. Lalović, G. Paić, I. Slaus, and P. Tomaš, *Phys. Rev. Letters* **14**, 444 (1965); J. D. Anderson, C. Wong, J. W. McClure, and B. A. Pohl, *ibid.* **15**, 66 (1965); A. M. Baldin, *Phys. Letters* **17**, 47 (1965); S. T. Thornton, J. K. Blair, C. M. Jones, and H. B. Thomas, *Phys. Rev. Letters* **17**, 701 (1966); J. A. Cookson, *Phys. Letters* **22**, 612 (1966); B. Antolković, M. Cerineo, G. Paić, P. Tomaš, V. Ajdacić, B. Lalović, and W. T. H. Van Oers, *ibid.* **23**, 477 (1966); H. H. Forster, J. Hakhikian, and C. C. Kim, in *Proceedings of the International Conference on Nuclear Physics, Gallinburg, Tennessee, 1966* (Academic Press Inc., New York, 1967), p. 1025; V. Valkovic, S. T. Emerson, W. R. Jackson, and G. C. Phillips, *ibid.*, p. 989; R. F. Frosch, H. L. Crannell, J. S. McCarthy, R. E. Rand, R. S. Safrata, L. R. Suelzle, and M. R. Yearian, *Phys. Letters* **24B**, 54 (1967); R. E. Warner, J. S. Vincent, and E. T. Boschitz, *ibid.* **24B**, 91 (1967); P. G. Young, R. H. Stokes, and G. G. Ohlsen, *Bull. Am. Phys. Soc.* **13**, 569 (1968).

² C. C. Kim, S. M. Bunch, D. W. Devins, and H. H. Forster, *Phys. Letters* **22**, 314 (1966).

³ The results of the present experiment have already been briefly reported; see R. E. Brown and D. K. Olsen, *Bull. Am. Phys. Soc.* **12**, 892 (1967); D. K. Olsen and R. E. Brown, John H. Williams Laboratory of Nuclear Physics Annual Report, 1967, p. 66 (unpublished).

⁴ M. D. Mancusi, C. M. Jones, and J. B. Ball, *Phys. Rev. Letters* **19**, 1449 (1967).

⁵ S. M. Austin, W. Benenson, and R. A. Paddock, *Bull. Am. Phys. Soc.* **12**, 16 (1967).

⁶ ORTEC, Series 600, 17-in. diam.

particles of interest would stop in it while charge-1 particles would pass through it. Tests of these detectors carried out at low bias voltage with a ThC α -particle source showed that their energy resolution was sufficiently good for the present experiment. During data taking, these three detectors were mounted behind rectangular, tantalum collimators fixed to one turntable of the scattering chamber. They were positioned 14 cm from the target and were separated in lab angle by 5°. Each collimator subtended a solid angle of 1.1 msr and subtended an angle in the reaction plane of 0.65°.

The detector assembly used to monitor elastically scattered protons was a two-detector stack consisting of 1- and 2-mm-thick, transmission-mounted surface-barrier detectors connected in parallel. This assembly subtended a solid angle of 0.30 msr and was normally placed at 90° to the incident beam.

C. Electronic Apparatus

Standard techniques were used to amplify and shape the signals from each of the four detector assemblies. These signals were then digitized in four separate analog-to-digital converters, and the digital information was fed to the direct-memory unit,⁷ an interface which communicates with the memory of a CDC 3100 computer. Four pulse-height spectra of 1024 channels each were thereby recorded simultaneously, and, once in the memory, the data could be manipulated with FORTRAN programs, displayed on an oscilloscope, analyzed with a light pen, and graphed with an automatic plotter.

D. Li Targets

Lithium targets were made by enclosing evaporated, 99.3% isotopically pure Li⁶ between a commercial nickel foil and a sputtered nickel surface. Use of this type of target (a) allows targets to be transferred from a single target-making apparatus to any one of several scattering chambers without special apparatus at each chamber, (b) allows the targets to be used, without change in composition, in scattering chambers operating at pressures of about 10⁻⁵ Torr, and (c) alleviates the waste of accelerator time which sometimes occurs when targets are prepared *in situ*. Details of the techniques and procedures used in the preparation of these targets are given elsewhere.⁸⁻¹⁰ Target compositions were measured by means of proton elastic scattering; the details are given in Ref. 8. Table I lists the composition of the lithium target used to obtain the data

TABLE I. Lithium target composition in units of 10¹⁸ nuclei/cm². The lithium is 99.3% Li⁶.

H	Li	C	O	Ni
4.0	43.5	0.9	5.5	2.8

presented here. The indicated carbon concentration is that near the beginning of the data-taking period. At the end of this period the carbon concentration had increased by only 7%. This target was perfectly adequate in terms of the ratio of the number of Li⁶ nuclei to the numbers of other nuclei. In fact, spectral positions of discrete α -particle groups from (p,α) reactions produced by oxygen in the target served as useful checks on the energy calibration of the detection system. Subsequent to this experiment, further improvements in target fabrication technique have resulted in the production of targets having about the same amount of lithium and carbon as the target of Table I, but having about five times less oxygen and hydrogen.¹⁰

III. PROCEDURE AND RESULTS

A. Experimental Method

During collection of (p,α) data, the apparatus described in Sec. II was employed in the following manner. For each angular setting of the scattering-chamber turntable, three α -particle spectra at angles separated by 5° (lab) were measured simultaneously with a proton-monitor spectrum at 90° (lab). The 90° yield of protons elastically scattered from Li⁶, C, O, and Ni provided a continuous monitor of both relative and absolute target composition and thickness. A sample monitor spectrum is shown in Fig. 1. The three α -particle detectors were operated at bias voltages low enough to result in thin sensitive regions. This was done because then protons, deuterons, and tritons of even relatively low energy would pass through this region and lose only a fraction of their energy therein, whereas α particles of the same energy would stop in the sensitive region and deposit their full energy. When the detectors are operated in this manner, their pulse-height spectra exhibit sharp edges corresponding to the deposition of energy in the detector by particles whose range is equal to the thickness of the sensitive region. No particle type can produce a pulse height greater than that of its associated edge, no matter what the particle energy, and essentially no information on the α -particle continuum can be obtained for pulse heights below the highest such edge. Except at the three most forward angles, where Li⁶ recoil particles were present, the deuteron edge gave the lower limit to the energy of α particles which could be clearly observed, and this in turn gives the upper limit to the possible He³ excitation which could have been observed.

A lower limit to the α -particle detector bias voltage is required so that the energy deposited in the detector

⁷ R. K. Hobbie and R. W. Goodwin, Nucl. Instr. Methods **52**, 119 (1967); R. K. Hobbie, AEC Report No. COO-1265-44, 1966 (unpublished).

⁸ David K. Olsen, M. S. thesis, University of Minnesota, 1968 (unpublished).

⁹ David C. Weisser and David K. Olsen, John H. Williams Laboratory of Nuclear Physics Annual Report, 1967, p. 114 (unpublished).

¹⁰ David C. Weisser, Ph.D. thesis, University of Minnesota, 1968 (unpublished).

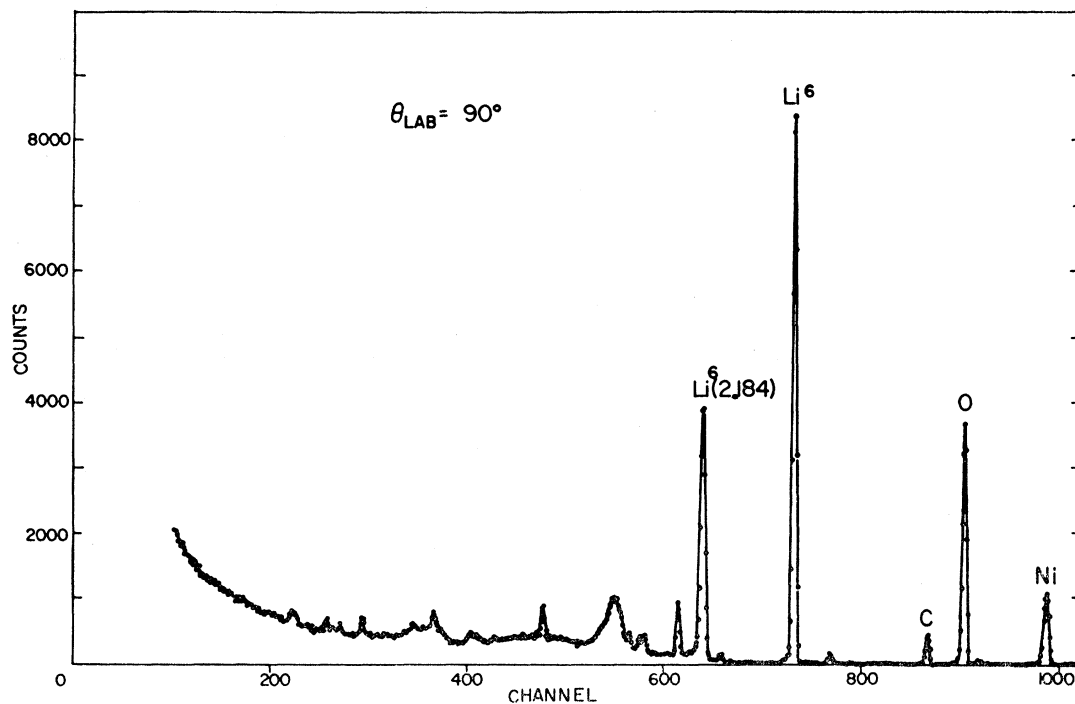


FIG. 1. Sample proton-monitor spectrum at 90° . The spectrum was obtained by 20.0-MeV proton bombardment of the lithium target of Table I. Labeled are proton groups elastically scattered from Ni, O, C, and Li^6 , and a proton group inelastically scattered from the 2.184-MeV state of Li^6 .

by He^3 particles from the strong reaction $\text{Li}^6(p, \text{He}^3)\text{He}^4$ (g.s.) should not overlap the energy deposited by the continuum α particles of interest. Therefore, by an adjustment of bias voltage at each angle, the sensitive region of the detector was made as thin as possible while still keeping a clear separation between the

passing He^3 particles and the start of the α -particle continuum at 5.49 MeV of excitation in He^3 .

Figure 2 shows a complete spectrum at 45° (lab) taken with an α -particle detector whose sensitive region was 160μ thick. Point 8 on the spectrum is the location of the deuteron edge and point 9 is that of the proton

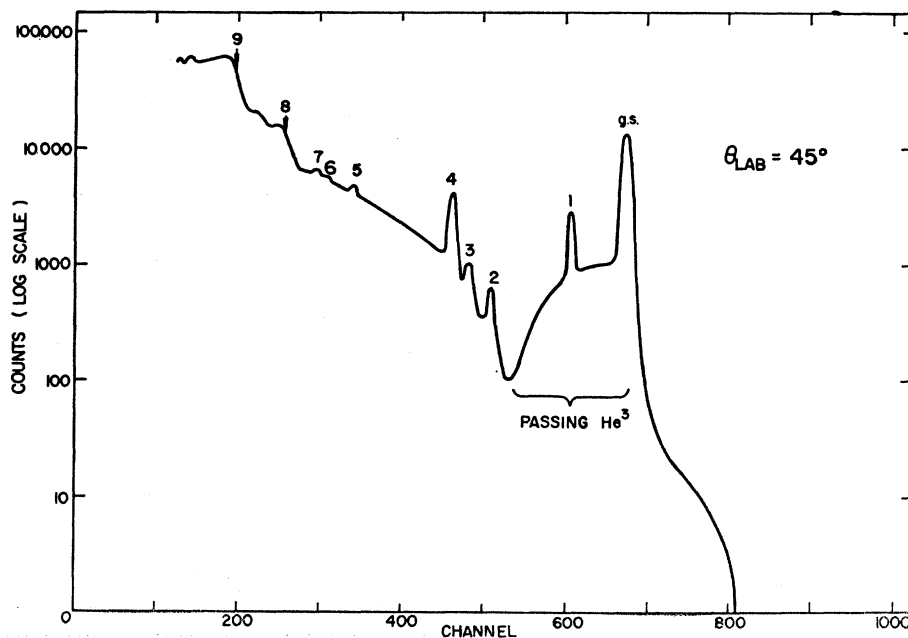


FIG. 2. Semilog plot of a spectrum at 45° measured with one of the three α -particle detectors. The peak labeled "passing He^3 " is produced by He^3 particles from the reaction $\text{Li}^6(p, \text{He}^3)\text{He}^4$ (g.s.) which pass through the sensitive region of the detector. The peak labeled "g.s." is produced by α particles from the $\text{Li}^6(p, \alpha)\text{He}^3$ (g.s.) reaction. The numbers label structure identified in Table II.

edge. No triton edge, which would occur at larger channel number than the deuteron edge, is seen. The base of the deuteron edge in Fig. 2 corresponds to a lab α -particle energy of 5.8 MeV, which in turn corresponds to a possible He^3 excitation of 13.7 MeV. Numbers 1–7 in Fig. 2 refer to spectral structure as identified in Table II. The identification is discussed in more detail in Sec. III B. The triton edge is absent from the spectrum because all the elements in the target, with the exception of Ni, have large negative Q values for (p,t) reactions. Furthermore, the triton yield from a pure nickel target containing approximately the same number of nickel atoms as the lithium target was measured and found to be very small. Similarly, with the exception of the above-mentioned $\text{Li}^6(p,\text{He}^3)\text{He}^4$ (g.s.) reaction, either large negative Q value or small production rate prohibits significant He^3 production from the elements in the target. Therefore, the energy region between the passing He^3 particles [from $\text{Li}^6(p,\text{He}^3)$] and the deuteron edge contains α particles almost entirely. In addition, the $\text{Ni}(p,\alpha)$ yield was measured separately and found to be very low, and therefore the observed continuum α particles come principally from the light elements in the target.

After the bias voltage on each α -particle detector was adjusted, an energy calibration was performed by recording a spectrum produced in each detector by a ThC α -particle source mounted on the target ladder. Next, the positions of the proton edges in the spectra were determined by scattering the incident protons from a thick tantalum target. This determination is essentially a measurement of the thickness of the sensitive region of each detector, a useful quantity to know when interpreting pulse-height distributions. After the bias-voltage adjustment, energy calibration, and thickness measurement, a (p,α) data run was taken with the lithium target.

Immediately after this data run, in which three simultaneous α -particle spectra were measured, spectra from a target or targets containing Ni, O, C, and H, but not Li, were measured without changing detector angles or electronic settings. This procedure allows a direct determination of the origin of spectral structure observed in the preceding data run with the lithium target. Early in the experiment three separate targets, one of polystyrene, one of Mylar, and one of pure nickel, were used for this purpose. However, it was later decided that a separate spectrum from each of these targets was not necessary for the identification of the spectral structure, and a single target, consisting of a mixture of nickel-oxide powder in a polystyrene binder, was used for the identification of structure during all subsequent data taking.

In summary, the following series of operations was normally carried out for each α -particle detector at each turntable angle: (i) detector bias-voltage adjustments, (ii) energy calibration with a ThC source, (iii) measurement of the thickness of the detector-

TABLE II. Identification of spectral structure. The numbers label structure in the figures.

Number	Identification
1	$\text{O}^{16}(p,\alpha)\text{N}^{13}$ (g.s.)
2	$\text{O}^{16}(p,\alpha)\text{N}^{13}$ (2.37)
3	$\text{C}^{12}(p,\alpha)\text{B}^9$ (g.s.)
4	$\text{O}^{16}(p,\alpha)\text{N}^{13}$ (3.51) and $\text{O}^{16}(p,\alpha)\text{N}^{13}$ (3.56)
5	$\text{O}^{16}(p,\alpha)\text{N}^{13}$ (6.38)
6	$\text{O}^{16}(p,\alpha)\text{N}^{13}$ (7.18)
7	$\text{O}^{16}(p,\alpha)\text{N}^{13}$ (7.42)
8	deuteron edge
9	proton edge

sensitive region, (iv) simultaneous measurement of three α -particle spectra and a proton-monitor spectrum produced by bombardment of the lithium target, and (v) a repeat of (iv) with the nickel-oxide-polystyrene target.

In Figs. 3 and 4 are shown, for several but not all angles measured, the portion of the α -particle spectrum which extends from the beginning of the continuum at 5.49-MeV excitation in He^3 up to the beginning of the deuteron edge (Li^6 recoil peak for 20° spectrum). Figure 3 shows the continua at 20° , 30° , and 40° (lab), and Fig. 4 shows the continua at 50° , 60° , and 70° (lab).

Some special data were also taken during which there were deviations from the above procedure. At the three most forward angles investigated (15° , 20° , and 25°), it was not the deuteron edge which placed a lower limit on the observed α -particle energy, but was instead a broad peak due to Li^6 recoil nuclei. Therefore, at these three angles spectra were measured with thin foils placed in front of the detectors. Since the energy loss of a Li^6 nucleus is greater than that of an equal-energy α particle, this procedure allowed the observation of α particles of a lower energy than otherwise, and hence observation of a higher possible He^3 excitation. Figure 5 shows the 25° data both with and without a foil in front of the detector. At 60° , 65° , and 70° additional spectra were measured with lower than normal bias voltage applied to the detectors. This caused the He^3 particles from the $\text{Li}^6(p,\text{He}^3)\text{He}^4$ (g.s.) reaction to fall onto the upper part of the α -particle continuum, but moved the deuteron edge to a significantly lower energy, and therefore allowed a higher possible He^3 excitation energy to be observed. Figure 6 shows the 65° data at both normal and reduced bias voltage. Table III lists the following information for each (p,α) spectrum measured: figure number if shown here, lab angle θ_{lab} for the spectrum, detector thickness t , maximum possible He^3 excitation energy $E_x(\text{max})$ which could have been observed, and a factor K which, when multiplied by the number of counts per channel in the figures, yields an approximate lab continuum cross section $\sigma_{\text{lab}}(\theta_{\text{lab}}, E_\alpha)$ in mb/sr MeV for the $\text{Li}^6(p,\alpha)$

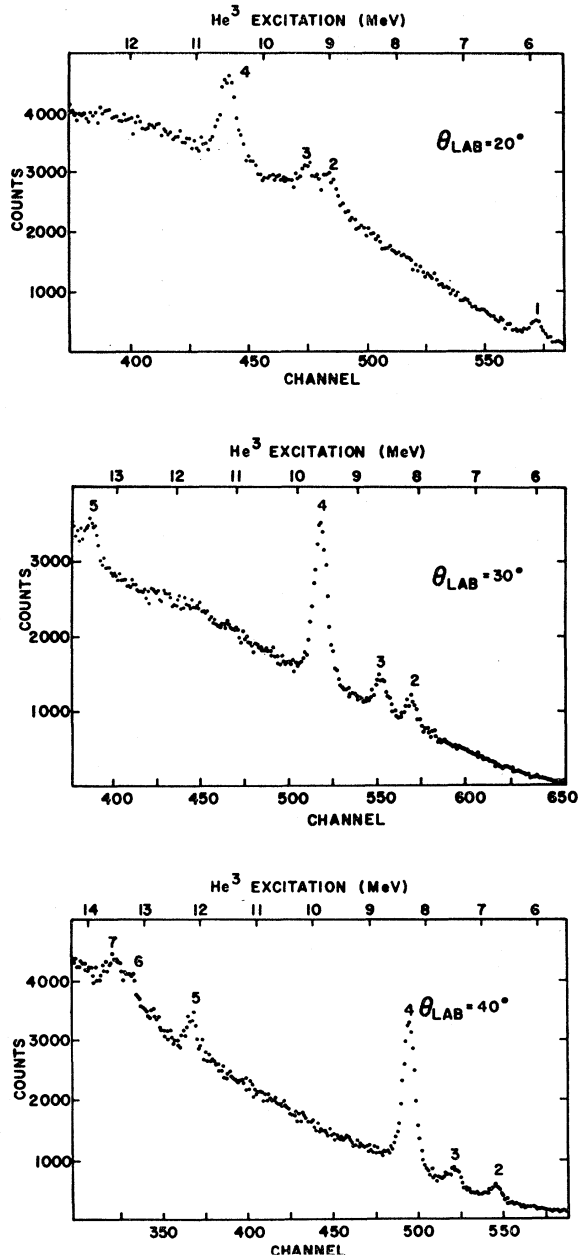


FIG. 3. Investigated portion of the $\text{Li}^6(p, \alpha)$ continuum at 20° , 30° , and 40° . The numbers label contaminant peaks, which are identified in Table II. Table III lists other parameters of interest.

reaction. No effort was made to determine K any more accurately than about $\pm 15\%$.

B. Identification of Structure

The identification of spectral peaks was made using three effects: (1) the kinematic energy change of the peaks with angle, (2) the peak positions as directly compared with those from the bombardment of a target or targets containing Ni, O, C, and H, but no Li, and (3) the number of counts in a peak as compared

with that expected from the known target composition. Effect (1) was readily observable and easy to use for identification because the relative nuclear masses involved made this effect large. The ThC energy calibration was verified at each angle using the kinematically calculated energy and experimentally observed channel number of the $\text{C}^{12}(p, \alpha)\text{B}^9$ and $\text{C}^{12}(p, \alpha)\text{B}^9(2.34)$ α -particle groups from the nickel-oxide-polystyrene target. The degree of consistency observed indicates an over-all accuracy of the energy calibration of ± 50 keV, which was more than adequate for the present experi-

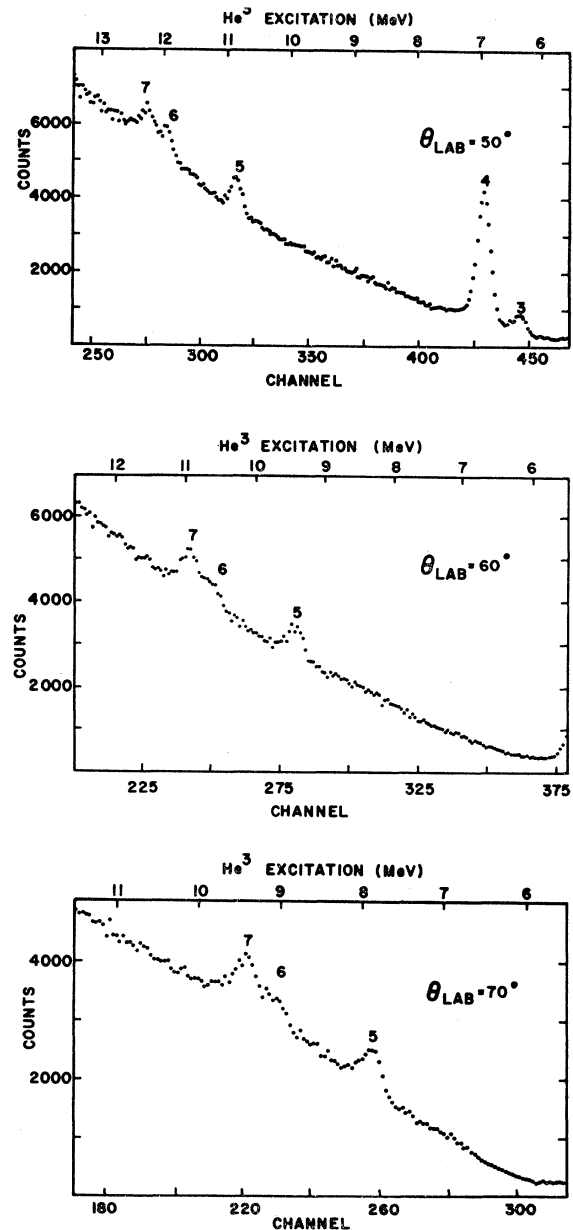


FIG. 4. Investigated portion of the $\text{Li}^6(p, \alpha)$ continuum at 50° , 60° , and 70° . The numbers label contaminant peaks, which are identified in Table II. Table III lists other parameters of interest.

ment. All the peaks were investigated by use of effect (1), and the change in lab energy with lab angle for each peak was consistent with its final identification in Table II. Care was taken to make all necessary corrections for the energy loss of the outgoing α particles in the target.

Identification of structure through effect (2) is consistent with the identification through effect (1), and some details of the use of effect (2) are mentioned in Sec. III A. Although the use of effect (3) yields results consistent with the use of effects (1) and (2), such identification is much less certain because of the errors involved in subtracting the large continuum from the observed peaks.

Spectra from a pure nickel target showed no triton edge and only very weak He^3 or α -particle groups. The cross section for these He^3 or α -particle groups from nickel was found to be so small that their contribution to events in the energy region of the $\text{Li}^6(p,\alpha)$ continuum was negligible. Similarly, the contribution to the continuum from the $\text{C}^{12}(p,\alpha)$ reaction leading to excited states of B^9 was negligible. In contrast, all the α -particle groups from the $\text{O}^{16}(p,\alpha)$ reaction leading to states in N^{13} below 7.42 MeV of excitation were seen

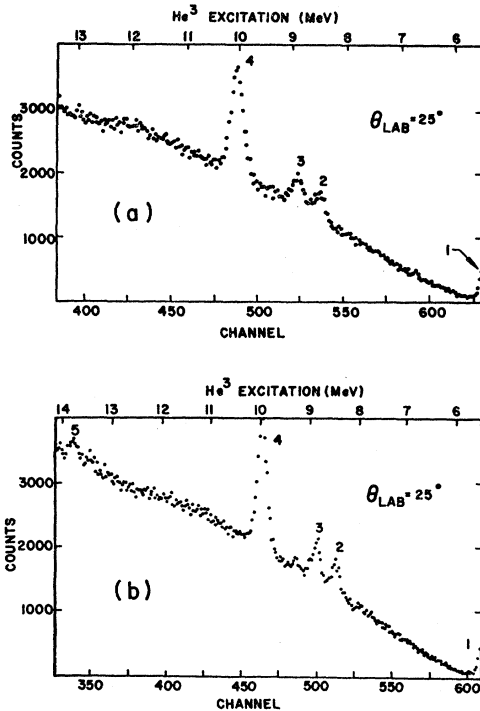


FIG. 5. Investigated portion of the $\text{Li}^6(p,\alpha)$ continuum at 25° . Spectrum (a) was measured under normal conditions (Sec. III A), and the low-channel cutoff was caused by the occurrence of the Li^9 -recoil peak (not shown). Spectrum (b) was measured with a $1.93\text{-}\mu$ nickel foil in front of the detector. This procedure degraded the energy of the Li^6 particles more than that of the low-energy α particles, thereby allowing a higher possible He^3 excitation to be observed. The numbers label contaminant peaks, which are identified in Table II. Table III lists other parameters of interest.

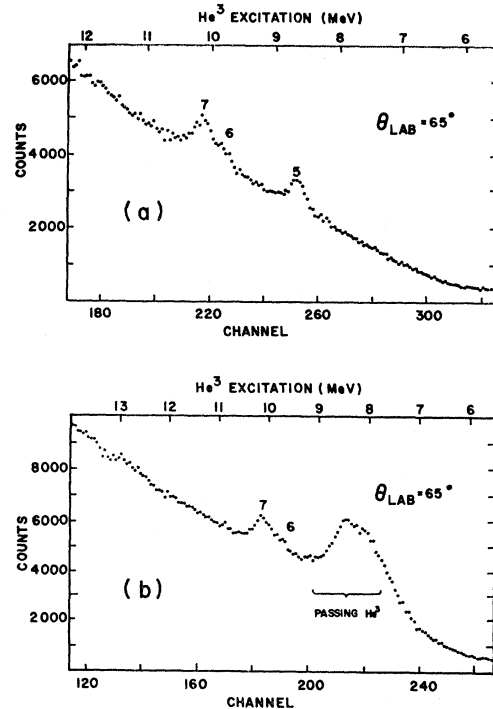


FIG. 6. Investigated portion of the $\text{Li}^6(p,\alpha)$ continuum at 65° . Spectrum (a) was measured under normal conditions (Sec. III A), and the low-channel cutoff was caused by the occurrence of the deuteron edge (not shown). Spectrum (b) was measured with the detector bias voltage reduced below that used during the spectrum-(a) measurement. This procedure unavoidably caused the He^3 particles from the $\text{Li}^6(p,\text{He}^3)\text{He}^4$ (g.s.) reaction, labeled "passing He^3 ," to fall on the upper part of the $\text{Li}^6(p,\alpha)$ continuum, but did lower the energy deposited by deuterons in the sensitive region of the detector, thereby allowing a higher possible He^3 excitation to be observed. The numbers label contaminant peaks, which are identified in Table II. Table III lists other parameters of interest.

superimposed on the α -particle continuum, with the sole exception of the level at 6.91 MeV in N^{13} . This level was not observed in any of the spectra.

IV. DISCUSSION AND CONCLUSION

Figures 3–6 and Table II show that all of the clearly observable structure in the α -particle spectra is identifiable with groups from the (p,α) reaction on target elements other than lithium, and therefore no clear structure from $\text{Li}^6(p,\alpha)$ is seen. The same conclusion is true for the spectra listed in Table III but not illustrated in this paper. A close inspection of the spectra at 20° , 25° , and 30° (Figs. 3 and 5), however, reveals a very slight, broad, hump near 11- to 12-MeV excitation in He^3 . Several possibilities have been considered for the origin of this broad structure. For instance, α particles from $\text{C}^{12}(p,\alpha)$ are energetically allowed to occur in this region of the spectrum; however, direct measurement showed that the amount of carbon in the lithium target (Table I) was much too small to have caused this broad structure. Another process for

TABLE III. Several parameters for measured $\text{Li}^6(p,\alpha)$ spectra. Figure numbers are given for the illustrated spectra, the lab angle θ_{lab} is given in deg, the thickness t of the sensitive region of the detector is given in μ , the maximum possible He^3 excitation $E_z(\text{max})$ observable on each spectrum is given in MeV, and K is a conversion factor, accurate to $\pm 15\%$, which will yield the lab continuum cross section in mb/sr MeV when multiplied by the number of counts per channel.

Fig.	θ_{lab}	t	$E_z(\text{max})$	K
...	15°	260	12.9	...
...	15°	260	13.8 ^a	...
3	20°	240	12.9	1.2×10^{-3}
...	20°	240	14.0 ^a	...
5	25°	230	13.4	1.3
5	25°	230	14.1 ^a	1.3
3	30°	220	13.7	1.2
...	35°	190	13.9	...
3	40°	180	14.3	1.2
...	45°	160	13.7	...
4	50°	140	13.4	0.78
...	55°	100	12.9	...
4	60°	110	12.6	0.66
...	60°	90	13.6 ^b	...
6	65°	100	12.2	0.63
6	65°	50	14.0 ^b	0.47
4	70°	90	11.5	0.66
...	70°	60	12.8 ^b	...
...	75°	80	11.0	...
...	80°	60	11.0	...
...	85°	50	10.1	...

^a Thin foil in front of detector.

^b Passing He^3 on α continuum.

producing α particles is the two-stage reaction $\text{Li}^6(p,p')\text{Li}^{6*}(2.18) \rightarrow \alpha + d$. Figure 1 indicates that the first step in this sequence proceeds with appreciable probability at 20.0-MeV incident proton energy. The α particles from this two-stage reaction enter a fixed-angle detector with energies varying from zero up to some maximum value E_{max} . Often such a two-stage contribution to a continuum will manifest itself through a rapid change in slope of the continuum at an energy E_{max} . A computation¹¹ of E_{max} shows that it is too large for the broad structure near 11- to 12-MeV excitation to be due to the onset of this two-stage reaction. For example, at 30° an α particle with energy E_{max} would fall on the spectrum at 8.8-MeV He^3 excitation. The two-stage reaction $\text{Li}^6(p,d)\text{Li}^5 \rightarrow \alpha + p$ has an even larger E_{max} , and therefore is also eliminated as a cause of the observed broad structure. A lower E_{max} is obtained if the state $\text{Li}^{6*}(2.18)$ can break up with significant probability into $\alpha + d^*$, where d^* represents the virtual state of the deuteron. However, a kinematic computation for this two-stage reaction leading to d^* yields an E_{max} for the α particle, which is too low to be consistent with the observed spectral position of the broad structure. With regard to the possibility that the structure is due to the existence of a broad state in He^3 , we note that because this structure is visible only weakly and at only a few angles, and because it is

¹¹ Computer program written by Russell K. Hobbie.

TABLE IV. Upper limit to the lab differential cross section in $\mu\text{b/sr}$ for the excitation of He^3 states with a natural width of 0.9 MeV (c.m.).

θ_{lab}	He^3 excitation (MeV)			
	8.0	10.0	12.0	14.0
20°	200	260	300	350
40°	130	170	220	290
60°	100	140	190	...
80°	90	120

broad, it was not possible to determine whether or not it remains at constant He^3 excitation as the detector angle is varied. Therefore, one cannot assert that the structure is due to a state in He^3 . On the basis of the information obtained in the present experiment, such an assertion would be largely conjecture.

Upper limits to the lab differential cross section for the formation, in the $\text{Li}^6(p,\alpha)$ reaction at 20.0 MeV, of He^3 states having a natural width of 0.9 MeV (c.m.) have been determined from our data. This upper limit varies from spectrum to spectrum, and within each spectrum varies with observed α -particle energy. Table IV lists several of these upper limits as a function of θ_{lab} and He^3 excitation energy. These upper limits do not apply to those portions of the continua on which there are contaminant peaks. The presence of these peaks will not be likely to cause He^3 excited states to be missed, because a peak due to a He^3 excited state would move very rapidly in lab energy with angle compared to a contaminant peak. For example, at 45° a change of 5° would move a peak due to a He^3 state from a position where it completely overlaps a contaminant peak to a position where it is almost completely separated from the contaminant peak.

In conclusion, the $\text{Li}^6(p,\alpha)$ continuum produced by 20.0-MeV protons has been examined for structure due to He^3 excited states. Lab angles investigated varied from 15° to 85° in increments of 5°, and the maximum possible observable He^3 excitation varied from 14.3 MeV at 40° to 10.1 MeV at 85°. No clear structure was found which could be attributed to the formation of He^3 excited states. Upper limits to the differential cross section for forming such states are given in Table IV.

ACKNOWLEDGMENTS

We wish to thank all the personnel at the John H. Williams Laboratory of Nuclear Physics for their help during the course of this experiment. In particular, we acknowledge the assistance of Clarence G. Jacobs in data taking and of John E. Anderson in designing the detector mounts and collimators. Special thanks are expressed to David C. Weisser, whose diligent efforts in developing target fabrication techniques were invaluable to us.